Evidence for the a_1 meson being a difficult messenger for the restoration of chiral symmetry

Sascha Vogel and Marcus Bleicher

Institut für Theoretische Physik, J. W. Goethe-Universität, Max-von-Laue-Straße 1, D-60438 Frankfurt am Main, Germany

(Received 23 October 2007; revised manuscript received 12 November 2008; published 31 December 2008)

We perform a theoretical analysis of the a_1 resonance mass spectrum in ultrarelativistic heavy ion collisions within a hadron/string transport approach. Predictions for the a_1 yield and its mass distribution are given for the GSI-FAIR and the critRHIC energy regime. The potential of the a_1 meson as a signal for chiral symmetry restoration is explored. In view of the latest discussion, we investigate the decay channel $a_1 \to \gamma\pi$ in detail and find a strong bias toward low a_1 masses. This apparent mass shift of the a_1, if observed in the $\gamma\pi$ channel, might render a possible mass shift due to chiral symmetry restoration very difficult to disentangle from the decay kinematics.

DOI: 10.1103/PhysRevC.78.064910 PACS number(s): 25.75.Dw, 11.30.Rd, 13.25.Jx, 24.10.Lx

One of the main goals of relativistic heavy ion physics is to reach densities and temperatures high enough to restore chiral symmetry [1]. Chiral symmetry is a symmetry of quantum chromodynamics, which is exact if quark masses are zero and approximate if quark masses are small. It is spontaneously broken in nature, but expected to be restored at sufficiently high densities and temperatures. The restoration of chiral symmetry implies a change in the spectral functions of vector mesons (e.g., the ρ meson) and leads to a degeneracy of the spectral functions of the ρ and its chiral partner, the a_1 meson. This means that the masses of the chiral partners become equal in the case of full chiral symmetry restoration or approach each other in the case of a partial restoration of the symmetry.

Especially the recently observed broadening of the ρ meson spectral function by the NA60 Collaboration and the corresponding dilepton mass spectrum have been interpreted as a signal of chiral symmetry restoration [2–6]. In fact, the NA60 Collaboration measured the ρ meson spectral function in In + In systems at the highest SPS energy of 158 A GeV and observed a deviation from the vacuum Breit-Wigner distribution [7]. This has triggered various theoretical investigations [8–10]. In summary these studies suggest that some in-medium effects must be considered, but a conclusive interpretation of the data is still under discussion.

Also the HADES Collaboration has recently presented first results on dielectron spectra in light systems at low beam energies (C + C at 2 A GeV) [11]. Here a deviation from the hadronic vacuum cocktail is visible in the mass region of 500 to 700 MeV. This has been discussed as a possible observation of partial chiral symmetry restoration and the resulting change in the ρ meson spectral function. Similar data have also been measured by the CERES experiment at CERN in massive nuclear reactions at high energy [12]. Despite the ongoing experimental and theoretical efforts, there are numerous effects that must be taken into account for a full understanding of the data. Thus, it is questionable that a mass shift of the ρ meson alone can be regarded as a "smoking gun" signal of chiral symmetry restoration [13,14]. Therefore, a more robust signature of chiral symmetry restoration is needed.

Theory predicts that in the case of a full restoration of chiral symmetry the spectral functions of the ρ meson and its chiral partner, the a_1 meson, become degenerate. The important point is that this statement is independent of any mass shift or broadening. Thus, it has been proposed over the recent years to measure the a_1 mass spectrum in a hot and dense medium and compare it to the mass spectrum of the ρ meson [15,16]. If the degeneracy would be observed it is expected to serve as an unambiguous experimental signal for the detection of chiral symmetry restoration in the hot and dense medium.

In this article we argue that the measurement of the a_1 (1260) meson may not result in straightforward insights for the understanding and the detection of the chirally restored phase. We discuss the decay kinematics of the a_1 meson and argue that an apparent mass shift or, respectively, a broadening of the mass spectrum may originate from mass dependent branching ratios. This effect is not unique to heavy ion reactions, but is qualitatively independent of energy and system size. Furthermore, we predict a_1 mass spectra for Au + Au and $p + p$ collisions at 20 and 30 A GeV beam energy. The $p + p$ calculations can serve as a vacuum reference. These systems and energies are experimentally accessible at FAIR, NA61, and the critRHIC program in the near future.

For our calculations we utilize the UrQMD (v2.3) model [17], a nonequilibrium transport approach, which relies on the covariant Boltzmann equation. All cross sections are calculated by the principle of detailed balance and the additive quark model or are fitted to available data. UrQMD does not include any explicit in-medium modifications or effects to describe the restoration of chiral symmetry. The model allows the study of the full space time evolution of all hadrons, resonances, and their decay products in hadron-hadron or nucleus-nucleus collisions. This permits exploration of the emission patterns of resonances in detail and insight into their origins and decay channels. For previous studies of resonances within this model see Refs. [13,18–21]. For further details about the UrQMD model the reader is referred to Refs. [22,23].

Experimentally, the reconstruction of resonances is challenging. One often applied technique is to reconstruct the invariant mass spectrum for single events. Then, an invariant mass distribution of mixed events is generated (here, the particle pairs are uncorrelated by definition). The mixed event distribution is subtracted from the invariant mass spectrum of the single (correlated) events. As a result one obtains the mass distributions and yields (after all experimental corrections)

of the resonances by fitting the resulting distribution with a suitable function (usually a Breit-Wigner function peaked around the pole mass of the respective resonance) [24,25]. If a daughter particle (re-)scatters before reaching the detector the signal for the experimental reconstruction is lost. Especially for strongly interacting decay products this effect can be sizable. In addition, because of the statistical nature of the reconstruction, detailed information on the particle properties and their origin is difficult to obtain. Also possible deviations from a Breit-Wigner distribution can be overseen because of a possible dependence on the background subtraction.

Thus, we apply a different technique for the extraction of resonances from the model. We follow the individual decay products of each decaying resonance (the daughter particles). If the daughter particles do not rescatter in the further evolution of the system, the resonance is counted as "reconstructable." The advantage of this method is that it allows us to trace back the origin of each individual resonance to study their spatial and temporal emission pattern. It also allows us to explore the reconstruction efficiency in different decay branches.

The decay channels of the a_1 meson have not been fully experimentally investigated and details of the branching ratios are unknown [26]. However, a most promising decay channel for the investigation of the restoration of chiral symmetry seems to be the decay $a_1 \to \gamma\pi$, due to the fact that the photon does essentially not interact with the surrounding (hadronic) medium. A study of all other decay channels would imply the need to study three particle correlations or, respectively, correlations between resonances and stable particles, which is very tedious, if not impossible in large systems. However, see also the discussion at the end of this article. Thus, experimentally, the $a_1 \to \gamma\pi$ channel seems the only feasible candidate to measure the a_1 meson in heavy ion collisions, even though the pion undergoes final state interactions.

One problem is that the branching ratio into this certain decay channel is still not very well known. For the present study, we employ a partial width of $\Gamma_{a_1\to\gamma\pi} = 640$ keV, resulting in a branching ratio of $BR_{a_1\to\gamma\pi} = 0.0016$, in line with Ref. [26]. Further experimental studies in elementary systems would be helpful to obtain more precise quantitative results in theoretical investigations.

In Fig. 1 the mass spectrum of the a_1 meson for $p + p$ collisions at 20 and 30 A GeV obtained from the UrQMD calculation is shown. One observes a clear peak around the pole mass of the a_1 meson. Note that this mass spectrum is narrower than the one obtained experimentally from τ decays [27], and we also like to refer to Ref. [28] for a detailed discussion of the a_1 spectral shape.

In Fig. 2 the mass spectrum of a_1 mesons for central ($b \leqslant 3.4$ fm) Au + Au collisions at 20 (solid line) and 30 A GeV (dotted line) as obtained from UrQMD calculations is depicted. As in the $p + p$ case, one observes a peak around the pole mass (although slightly shifted to lower masses for kinematic reasons discussed in Ref. [20]).

What happens now if one explicitly employs a trigger on the decay channel $a_1 \to \gamma\pi$ that seems most suitable for the study of the a_1 in heavy ion reactions? As discussed in Refs. [22,29] the branching ratios of resonances depend on the mass of the decay products. The total decay width $\Gamma_{\text{tot}}(M)$ of a resonance

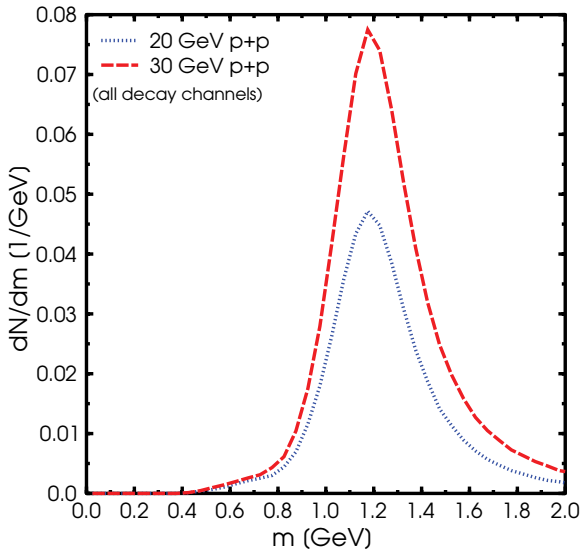

FIG. 1. (Color online) Mass distribution of a_1 mesons in proton-proton collisions at $E_{\text{lab}} = 20$ (dotted line) and 30 A GeV (dashed line) as obtained from UrQMD calculations. No trigger on a specific decay channel has been applied.

is defined as the sum of all partial decay widths and depends on the mass of the excited resonance:

$$\Gamma_{\text{tot}}(M) = \sum_{\text{br}=\{i,j\}}^{N_{\text{br}}} \Gamma_{i,j}(M), \tag{1}$$

where $\Gamma_{i,j}(M)$ is the partial decay width, M is the mass of the resonance and the summation over N_{br} denotes a summation over all possible decay channels. The partial decay widths $\Gamma_{i,j}(M)$ for the decay into the exit channel with particles i and

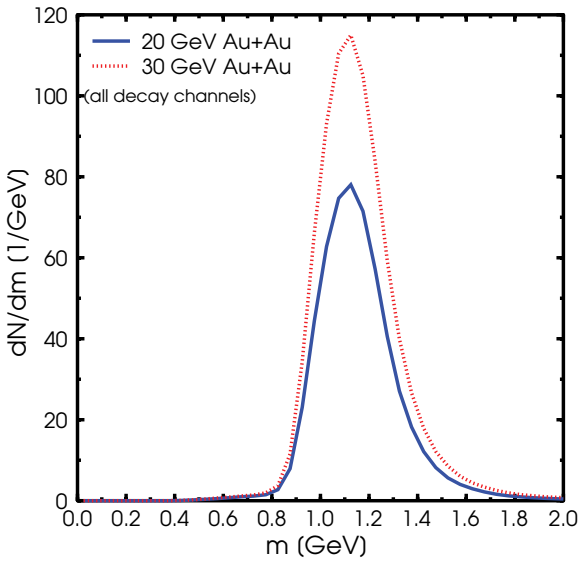

FIG. 2. (Color online) Mass distribution of a_1 mesons in central Au + Au collisions ($b \leqslant 3.4$ fm) at 20 (solid line) and 30 A GeV (dotted line) as obtained from UrQMD calculations.

j is given by [22,29]

$$\Gamma_{i,j}(M) = \Gamma_R^{i,j} \frac{M_R}{M} \left(\frac{\langle p_{i,j}(M) \rangle}{\langle p_{i,j}(M_R) \rangle} \right)^{2l+1} \frac{1.2}{1 + 0.2 \left(\frac{\langle p_{i,j}(M) \rangle}{\langle p_{i,j}(M_R) \rangle} \right)^{2l}}, \tag{2}$$

here M_R denotes the pole mass of the resonance, $\Gamma_R^{i,j}$ its partial decay width into the channel i and j at the pole, and l the decay angular momentum of the exit channel. $\langle p_{i,j}(M) \rangle$ denotes the momentum of the decay products in the center of momentum frame. Note, however, that this equation does not include most sophisticated quantum mechanical effects but serves as a well known and often assumed phenomenological description of the underlying mass dependence of hadronic decays. Implementation of the full quantum mechanical description is beyond the scope of this work and has to our knowledge not been included in any other transport models.

Figure 3 shows the branching ratio of the a_1 meson as a function of the mass of the a_1 as obtained from UrQMD calculations, wherein the definitions (1) and (2) are implemented including the finite width of decay particles. Solid squares depict the branching ratio of a_1 mesons into the exit channel $\rho\pi$, whereas open squares depict the branching ratio into $\gamma\pi$. Also shown is a normalized breit-wigner distribution (solid line) and the normalized mass spectrum of the a_1 meson as obtained from proton-proton collisions at 20 A GeV from UrQMD. One observes that at masses lower than 600 MeV the decay channel of $a_1 \to \gamma\pi$ dominates because the decay channel into $\rho\pi$ is kinematically suppressed. At masses greater than 600 MeV the $\rho\pi$ decay channel is dominantly populated and the contribution from the $\gamma\pi$ channel becomes less important. Depicted in Fig. 3 are only two of the possible decay channels listed in Ref. [26]. All other exit channels consist of even heavier decay products.

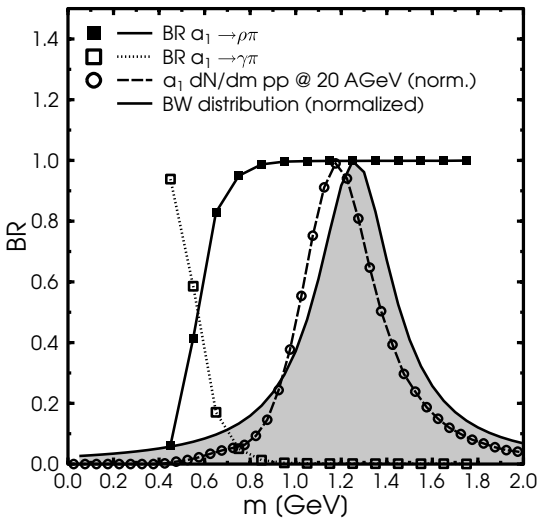

FIG. 3. Mass dependent branching ratios for the a_1 meson with the two exit channels of $\gamma\pi$ and $\rho\pi$ as calculated from UrQMD. Solid squares depict the branching ratio of a_1 mesons into the exit channel $\rho\pi$, whereas open squares depict the branching ratio into $\gamma\pi$. Below a mass of 600 MeV the decay channel $a_1 \to \rho\pi$ is kinematically suppressed and the channel $a_1 \to \gamma\pi$ dominates. At masses above 600 MeV the branching ratio into $\rho\pi$ increases steeply. The grey shaded area depicts a normalized Breit-Wigner distribution around the a_1 pole mass, whereas the circles depict the normalized mass spectrum of the a_1 meson as obtained from UrQMD calculations for $p + p$ collisions at 20 A GeV.

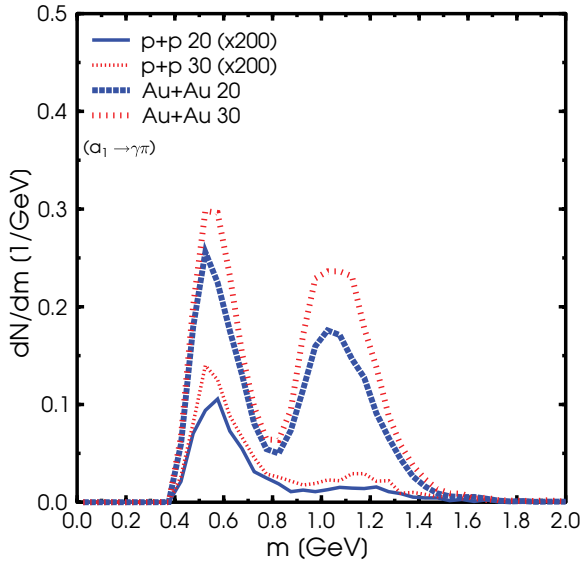

FIG. 4. (Color online) Mass distribution of a_1 mesons that can be reconstructed in $\gamma\pi$ correlations in nucleus-nucleus and proton-proton collisions at 20 and 30 A GeV. Note that the $p + p$ curves have been multiplied by a factor of 200 for better visibility.

After these semiquantitative discussions, it is clear that a nontrivial a_1 mass spectrum has to be expected in the full UrQMD calculation, if a trigger on the $\gamma\pi$ exit channel is employed. By folding the branching ratio of $a_1 \to \gamma\pi$ and the Breit-Wigner distribution shown in Fig. 3 one expects a distorted mass spectrum. Let us therefore test this effect within the full transport model calculation.

Figure 4 shows the mass spectrum for those a_1 mesons that can be (in principle) reconstructed in the $a_1 \to \gamma\pi$ decay channel. The thick lines depict the results for Au + Au collisions at 20 or 30 A GeV. The thin lines depict the mass spectrum as obtained from $p + p$ collisions at the same energies. Note that the $p + p$ curves have been scaled up for better visibility.

One observes a clear double peak structure, with one peak centered around the pole mass and one peak in the range of 400–600 MeV. This enhancement is seen in both the Au + Au and the $p + p$ case, indicating that it may not be a unique effect seen in heavy ion collisions. Thus, a possible a_1 mass shift due to chiral symmetry restoration might be difficult to distinguish from a scenario without mass shift but including mass dependent branching ratios.

Another caveat to the detection of the chirally restored phase is the underlying baryon density distribution of the event. Although the photon does not underlie hadronic interaction, the pion still does. Thus it is important to investigate the density profile the decayed a_1 mesons originate from. The baryon density is averaged over all hadron positions and is calculated locally in the rest frame of the baryon current as

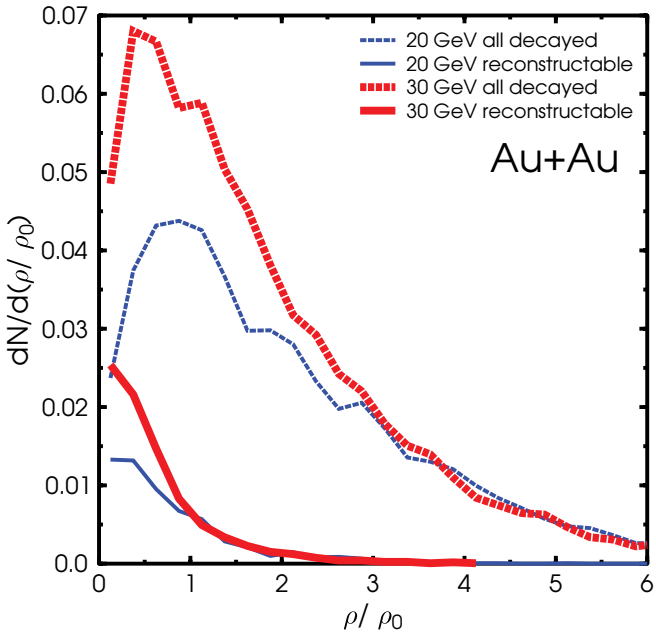

FIG. 5. (Color online) Baryon density distribution of a_1 mesons that decay into $\gamma\pi$ for central Au + Au collisions at 20 and 30 A GeV. Solid lines depict those a_1 mesons where the pion does leave the medium without further interaction; dashed lines depict all a_1 mesons that have decayed (without a trigger on being reconstructable). Thick lines depict Au + Au collisions at 30 A GeV beam energy; thin lines depict Au + Au collisions at 20 A GeV beam energy.

$\rho_B = j^0$ with $j^\mu = (\rho_B, \vec{0})$. Note that the maximal baryon density grows with increasing beam energy. Figure 5 depicts the density normalized to nuclear ground state density (ρ/ρ_0) of the point where the a_1 meson decayed into $\gamma\pi$. Solid lines depict the distribution for a_1 mesons where the pion is in principle reconstructable; i.e., it does not interact in the further evolution of the system. Dashed lines depict all a_1 mesons that have decayed into $\gamma\pi$.

One observes that reconstructable a_1 mesons originate from relatively low density areas (on the average they decay at a density of 0.63 (20 A GeV) to 0.8 (30 A GeV) ρ_0 in the case where the pion can be reconstructed).

Let us finally discuss the time and space the a_1 mesons decay. In Fig. 6 the a_1 meson mass spectrum is shown at different times during a Au + Au collision at 20 A GeV. The solid line depicts decay at times before 5 fm/c; the dotted line decays between 5 and 7 fm/c. The dashed-dotted line shows the integrated mass spectrum. For the other lines please refer to the plot's legend. One observes that the low mass part of the spectrum mainly originates from early times (below 7 fm/c). The a_1 production in this region is mainly driven by string decays, whereas at later times the production via $\rho\pi$ scattering sets in. The average center of mass energy of a string in a 20 A GeV $p + p$ collision is 2.635 GeV. Because one must conserve the baryon number at least 938 MeV are reserved for baryon production, leaving roughly 1.6 GeV for particle production. After allocating momenta (and the probable production of pions and the corresponding momenta), this leaves roughly several hundred MeV for resonance production.

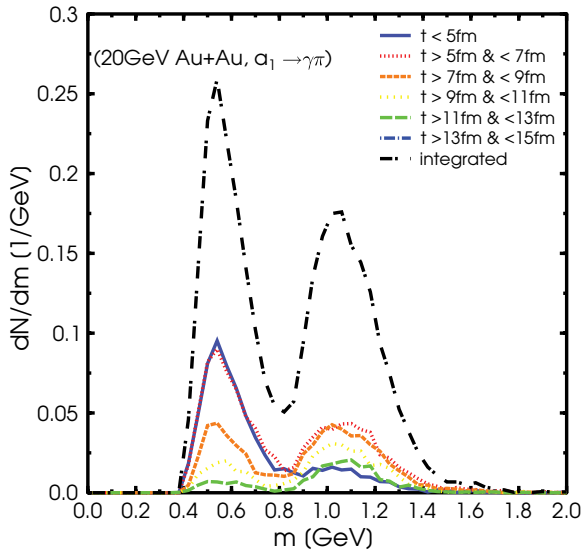

FIG. 6. (Color online) The a_1 meson mass spectrum for 20 A GeV Au + Au collisions evaluated during different times of the collision. The solid line depicts decays at times before 5 fm/c; the dotted line decays between 5 and 7 fm/c. The dashed-dotted line shows the integrated mass spectrum. For the other lines the reader is referred to the legend within the figure.

This effect leads to a slight shift in the a_1 meson mass spectrum, which results in the effects that have been discussed previously.

Figure 7 shows the points in space where reconstructable a_1 mesons decay. Solid circles depict reconstructable a_1 mesons without a mass cut, whereas squares depict those a_1 mesons with a mass of below 600 MeV. One observes that there is a slight bias toward the surface of the reaction zone. This is in

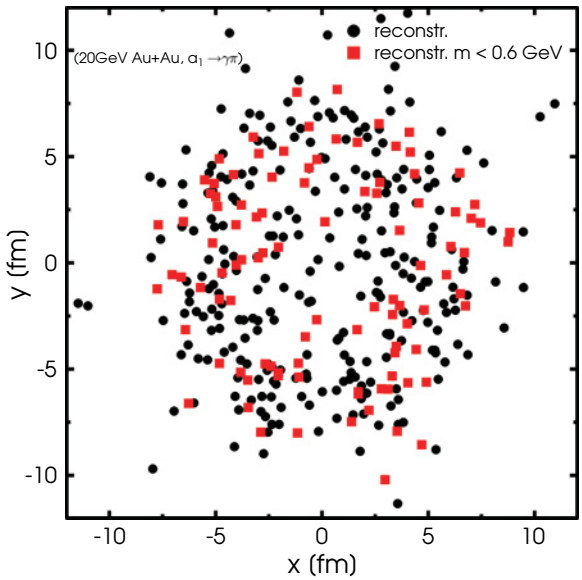

FIG. 7. (Color online) Scatterplot of the space-distribution (in x-y plane) of $a_1 \to \gamma\pi$ decays. Circles depict a_1 mesons that can be reconstructed experimentally (i.e., the pion does not undergo final state interaction). Squares depict the reconstructable a_1 mesons that have a mass of less than 600 MeV.

line with the observation that the density at those points is rather low, which enables the pion to leave the reaction zone undisturbed.

The fact that reconstructable a_1 mesons decay at low densities coupled with the decay kinematics discussed above might make the a_1 meson a difficult messenger of chiral symmetry restoration. Measuring the a_1 from a correlation of ρ mesons and pions might be more robust; however, it is experimentally even more demanding. One still faces the problem of the low density decays, but the $\rho\pi$ channel will avoid the problem of mass dependent branching ratios. But because the ρ meson decays mostly into pions it is required that one study three-particle correlations when analyzing the hadronic decay products. However, one might also consider the electromagnetic decay products of the ρ meson.

Indeed, the HADES (and later the CBM) experiment offer the unique possibility to measure correlations between ρ mesons and pions, where the ρ meson is reconstructed via the decay channel $\rho^0 \to e^+e^-$. These measurements might indeed provide a novel and up to now unexplored route to obtain insights into the transition from the chirally broken to the chirally restored phase.

In summary, we have presented a_1 mass distributions for $p + p$ and Au + Au reactions at $E_{\mathrm{lab}} = 20$ and 30 A GeV. It was shown that the reconstruction of the a_1 mass distribution in the $\gamma\pi$ channel is strongly biased toward low masses. This can be traced back to the strong mass dependence of the a_1 branching ratios. Thus, we conclude that a possible observation, e.g., at the planned GSI-FAIR facility or in a future critRHIC run, of a modified a_1 mass distribution measured in the $a_1 \to \gamma\pi$ exit channel cannot unambigiously signal an approach toward chiral symmetry restoration. However, a measurement in the $a_1 \to \rho\pi$ channel and a cross-check with results from the $a_1 \to \gamma\pi$ channel, as is possible with the HADES and CBM experiments, might lead to new information about the approach to chiral symmetry restoration.

ACKNOWLEDGMENTS

The computational resources have been provided by the Center for Scientific Computing, CSC, at Frankfurt University. We thank Volker Koch and Stefan Leupold for fruitful discussions. This work was financially supported by GSI and BMBF. S.V. thanks the Helmholtz foundation for additional financial support.

[1] S. A. Bass, M. Gyulassy, H. Stoecker, and W. Greiner, J. Phys. G: Nucl. Part. Phys. **25**, R1 (1999).
[2] V. Koch and G. E. Brown, Nucl. Phys. **A560**, 345 (1993).
[3] G. E. Brown and M. Rho, Phys. Rep. **269**, 333 (1996).
[4] W. Cassing, E. L. Bratkovskaya, R. Rapp, and J. Wambach, Phys. Rev. C **57**, 916 (1998).
[5] R. Rapp and J. Wambach, Adv. Nucl. Phys. **25**, 1 (2000).
[6] W. Cassing and E. L. Bratkovskaya, Phys. Rep. **308**, 65 (1999).
[7] R. Arnaldi *et al.* (NA60 Collaboration), Phys. Rev. Lett. **96**, 162302 (2006).
[8] J. Ruppert, T. Renk, and B. Muller, Phys. Rev. C **73**, 034907 (2006).
[9] J. Ruppert and T. Renk, Eur. Phys. J. C **49**, 219 (2007).
[10] H. van Hees and R. Rapp, Phys. Rev. Lett. **97**, 102301 (2006).
[11] G. Agakishiev (HADES Collaboration), Phys. Rev. Lett. **98**, 052302 (2007).
[12] D. Miskowiec (CERES Collaboration), Nucl. Phys. **A774**, 43 (2006).
[13] S. Vogel and M. Bleicher, Phys. Rev. C **74**, 014902 (2006).
[14] D. Schumacher, S. Vogel, and M. Bleicher, Acta Phys. Hung. A **27**, 451 (2006).
[15] R. Rapp, Nucl. Phys. **A725**, 254 (2003).
[16] Volker Koch, workshop on dileptons at CBM, GSI, 2007.
[17] H. Petersen, M. Bleicher, S. A. Bass, and H. Stocker, arXiv:0805.0567 [hep-ph].
[18] M. Bleicher and J. Aichelin, Phys. Lett. **B530**, 81 (2002).
[19] M. Bleicher, Nucl. Phys. **A715**, 85 (2003).
[20] M. Bleicher and H. Stoecker, J. Phys. G: Nucl. Part. Phys. **30**, S111 (2004).
[21] S. Vogel and M. Bleicher, arXiv:nucl-th/0505027.
[22] S. A. Bass *et al.*, Prog. Part. Nucl. Phys. **41**, 225 (1998).
[23] M. Bleicher *et al.*, J. Phys. G: Nucl. Part. Phys. **25**, 1859 (1999).
[24] J. Adams *et al.* (STAR Collaboration), Phys. Rev. C **71**, 064902 (2005).
[25] R. Witt, J. Phys. G: Nucl. Part. Phys. **34**, S921 (2007).
[26] W. M. Yao *et al.* (Particle Data Group), J. Phys. G: Nucl. Part. Phys. **33**, 1 (2006).
[27] S. Schael *et al.* (ALEPH Collaboration), Phys. Rep. **421**, 191 (2005).
[28] M. Wagner and S. Leupold, Phys. Lett. **B670**, 22 (2008).
[29] H. Sorge, Phys. Rev. C **52**, 3291 (1995).